MicroRNA-143 increases cell apoptosis in myelodysplastic syndrome through the Fas/FasL pathway both *in vitro* and *in vivo*

JIAQI CUI[1*], CHUNMEI WEI[1*], LINLI DENG[1], XINGYI KUANG[1], ZENGTIE ZHANG[2], CHRYSO PIERIDES[3], JIANXIANG CHI[3] and LI WANG[1]

[1]Department of Hematology, The First Affiliated Hospital of Chongqing Medical University, Chongqing 400016; [2]Department of Pathology, Xi'an Jiao Tong University Health Science Center, Xi'an, Shaanxi 710061, P.R. China; [3]Center for the Study of Haematological Malignancies, Karaiskakio Foundation, 2032 Nicosia, Cyprus

Received March 7, 2018; Accepted June 14, 2018

DOI: 10.3892/ijo.2018.4534

Abstract. Whilst the role of microRNA-143 (miR-143) in myelodysplastic syndrome (MDS) remains unclear, abnormally expressed microRNA-143 has been detected in many types of cancer tissues. In this study, we describe a cohort study for the verification of miR-143 expression, as well as the investigation of the molecular mechanisms of miR-143 in MDS/acute myeloid leukaemia (AML). In a series of experiments, miR-143 recombinant lentiviral vectors transformed into SKM-1 cells were either overexpressed or knocked down, and the results illustrated that the overexpression of miR-143 inhibited SKM-1 cell growth, arrested the SKM-1 cells in the G0/G1 phase, interfered with cell proliferation and induced cell apoptosis via the Fas/FasL pathway. Conversely, miR-143 knockdown induced a decrease in the apoptosis and promoted the proliferation of SKM-1 cells. Moreover, miR-143 was shown to suppress MLLT3/AF9 expression by binding to its 3'-UTR. Taken together, the findings of this study indicate that miR-143 may be a critical regulator of MDS/AML cell carcinogenesis, acting as a potent antitumour molecular target for the diagnosis or treatment of cancers associated with the abnormal expression of MLLT3/AF9, hence facilitating the development of potential therapeutics against MDS/AML.

Introduction

Myelodysplastic syndrome (MDS) presents a group of heterogeneous myeloid clones derived from haematopoietic stem cells (HSCs), usually manifesting as ineffective haematopoietic, refractory haematopoietic reduction and failure. With approximately 40% of patients with MDS developing acute myeloid leukaemia (AML), allogeneic HSC transplantation (HSCT) is the most commonly used treatment (1). Recent studies have greatly illuminated the genomic landscape of MDS (2); however, there is limited information on MDS pathogenesis and the developmental mechanisms. Thus, these aspects of MDS warrant clarification in order to improve patient prognosis. Accumulating evidence has indicated that the dysregulation of microRNAs (miRNAs or miRs) is involved in cancer proliferation, differentiation, apoptosis and metastasis, with miRNAs functioning as oncogenes or tumour suppressors, providing a promising method for the management of cancer (3,4). miR-143 expression changes, including both up- and downregulation, is frequently observed in various types of cancer. Whilst the downregulation of miR-143 causes it to act as a tumour suppressor in various types of tumour, including colorectal cancer (5-7), prostate cancer (8,9), gastric cancer (10,11), cervical cancer (12,13), nasopharyngeal carcinoma (14,15) and human osteosarcoma (16,17), miR-143 may also act as an anti-oncogene in T-cell leukaemia Jurkat cells (18). Various studies have demonstrated that miR-143 expression is downregulated in MDS (19-21); however the expression of miR-143 warrants further investigation by cohort studies. In addition, the molecular mechanisms of action of miR-143 in MDS/AML need to be further elucidated.

In the present cohort study, bone marrow (BM) samples from 33 patients with MDS and 11 healthy individuals were collected, with the healthy samples serving as the controls. To explore the molecular mechanisms of the disease, a series of experiments were performed in which miR-143 was either overexpressed or downregulated in *in vitro* recombinant lentiviral transfections of SKM-1 cells, a cell line used to transform MDS to AML harboring multiple karyotypic abnormalities, whilst lacking the 5q deletion. The effects of miR-143 on the proliferation, differentiation and apoptosis of SKM-1 cells were investigated and the *in vivo* vs. the *in vitro* effect of miR-143 was verified.

Correspondence to: Professor Li Wang, Department of Hematology, The First Affiliated Hospital of Chongqing Medical University, 1 Youyi Road, Yuzhong, Chongqing 400016, P.R. China
E-mail: liwangls@yahoo.com

*Contributed equally

Key words: microRNA-143, myelodysplastic syndrome, cell apoptosis, lentivirus, xenograft

Materials and methods

Samples and cell lines. Upon receiving written informed consent from all participants, a total of 44 BM samples (33 MDS/AML patient samples and 11 samples from healthy individuals) were obtained between October, 2012 to April, 2014 from the First Affiliated Hospital of Chongqing Medical University, Chongqing, China. The demographic characteristics of the patients included in this study are presented in Table I.

The SKM-1 cells [kindly provided by Professor Jianfeng Zhou of Tongji Medical College of Huazhong University of Science and Technology (Wuhan, China)] were cultured in RPMI-1640 (Gibco/Thermo Fisher Scientific, Waltham, MA, USA) with 10% heat-inactivated foetal bovine serum (FBS) (Gibco/Thermo Fisher Scientific) and were maintained in a humidified atmosphere of 5% CO_2 at 37˚C (22,23).

RNA isolation and reverse transcription-quantitative PCR (RT-qPCR). Mononuclear cells (MNCs) were isolated from the BM samples using Ficoll-Paque (GE Healthcare, MA, USA), and total RNA was extracted using RNAiso Plus (Takara, Dalian, China) according to the manufacturer's instructions. A commercially available cDNA synthesis kit (Takara) was used for cDNA synthesis. Quantitative PCR (qPCR) was performed using a CFX96 Touch™ Real-Time PCR Detection System (Bio-Rad, Hercules, CA, USA). The total reaction volume was 20 μl and was prepared as follows: SYBR Premix Ex Taq (10 μl), 0.8 μl of each primer (10 μmol/l), 2 μl of cDNA template and ddH_2O (6.4 μl). The RT-qPCR conditions were as follows: 95˚C for 3 min; 95˚C for 20 sec, followed by 62˚C for 50 sec repeated over 40 cycles. All primers were designed and synthesised by Novland (Novland Co., Ltd., Shanghai, China) and are presented in Table II. U6 was amplified as a reference for normalization and the results were analysed using the $2^{-\Delta\Delta Cq}$ method (24).

Construction of recombinant lentiviral vectors carrying hsa-miR-143 and hsa-miR-143-inhibitor. The miR-143 gene overexpression and knockdown lentiviral vector (LV) system contained GV217, pHelper 1.0 and pHelper 2.0 before packaging (GeneChem Co., Shanghai, China). The target sequences for the miR-143 overexpression lentiviral vector system were as follows: 5'-CGGCCGCGACTCTAGCAGAGCTGGAGAGGTGGAG-3' and 5'-ATAAGCTTGATATCGCAGGAAGGACAGAGTGTTTCC-3'. The primers for the miR-143-3p inhibition lentiviral vector were as follows: 5'-TGAGATGAAGCACTGTAGCTC-3' and 5'-GAGCTACAGTGCTTCATCTCA-3'. The production, purification and titration of the lentivirus were performed as previously described by Tiscornia *et al* (25). Three vectors for overexpression and downregulation were co-transfected into 293T cells [kindly provided by Professor Jianfeng Zhou of Tongji Medical College of Huazhong University of Science and Technology (Wuhan, China)] in serum-free media using Lipofectamine 2000 (Invitrogen Inc., Carlsbad, CA, USA). Following 8 h of incubation, the medium was changed to complete medium containing RPMI-1640 and 10% heat-inactivated FBS. The high-titre recombinant lentiviral vectors, LV-hsa-miR-143 and LV-hsa-miR-143-inhibitors, were harvested after 2 days of transfection.

RNA interference. The SKM-1 cells were seeded ($2x10^5$ cells/ml) in 6-well plates and infected with the lentivirus at a multiplicity of infection (MOI) of 10. The medium was replaced with fresh basic medium after 10 h. The infection efficiency was evaluated using a fluorescence microscope (SN:3832002173, Zeiss, Oberkochen, Germany) and the infection rate was detected by a flow cytometer (CytoFLEX, Beckman Coulter Corp., Tokyo, Japan) after 4 days.

Cell proliferation assays. Cell proliferation was determined using a Cell Counting kit-8 (CCK-8) assay (7Sea Biotech, Shanghai, China). Briefly, approximately $3x10^3$ cells/100 μl were seeded in 96-well plates and cultured at 37˚C for 1 day prior to transfection. The cells were then stably transfected with the lentivirus at an MOI of 10 for 10 h. The medium was replaced with fresh basic medium, and the cells were further incubated at 37˚C for 24, 48 and 72 h. Following incubation, CCK-8 reagent (10 μl) was added to each well, and the cells were incubated for an additional 2 h. Finally, the absorbance at 450 nm was measured by spectrophotometer (SN:1510-03523, Type:1510, Thermo Fisher Scientific, Vantaa, Finland).

Cell apoptosis and cell cycle assays. SKM-1 cell apoptosis was evaluated with an Annexin V-FITC/PI Apoptosis Detection kit (BD Biosciences, Heidelberg, Germany) according to the manufacturer's instructions using a flow cytometer (BD Biosciences, San Jose, CA, USA). For the cell cycle assay, the cells were harvested and fixed with 70% anhydrous alcohol for 4 h at 4˚C. The cells were then incubated with 100 μg/ml of propidium iodide (PI) for 30 min at room temperature. The cell cycle profiles were analysed using Multicycle software (Phoenix Flow Systems, San Diego, CA, USA).

Western blot analysis. Total protein from the SKM-1 cells and tumour tissues was harvested using RIPA lysis buffer supplemented with 1 μM PMSF (Beyotime, Shanghai, China), and the protein (40 μg) was loaded and separated on a 10% SDS-polyacrylamide gradient gel. The proteins were transferred onto polyvinylidene fluoride (PVDF) membranes with glycine transfer buffer and blocked for 1 h with 5% non-fat milk in PBS containing 0.1% Tween-20 (PBS-T). The blots were then incubated overnight at 4˚C with each primary antibody. The following primary antibodies were used in this study: Rabbit anti-human FasL (cat. no. YT0785), cleaved caspase-8 (cat. no. YT0011), cleaved caspase-3 (cat. no. YT0004) and cleaved caspase-9 (cat. no. YT0013) (Immunoway Biotechnology, Newark, DE, USA), each at a dilution of 1:500. Horseradish peroxidase-conjugated goat anti-rabbit IgG (cat. no. ZB-2306, ZSGB-BIO, Beijing, China) was used as the secondary antibody and GAPDH (cat. no. #5174, CST (Shanghai) Biological Reagents Co., Ltd., Shanghai, China) served as a loading control. The membranes were then washed 3 times with PBS containing 0.1% Tween-20 and incubated with the secondary antibody at a dilution of 1:7,000 for 2 h at room temperature. After washing with PBS-T (3x10 ml, 5 min each), the protein bands were visualised with an ECL kit (Beyotime), and the band intensity was analysed using Quantity One software (Bio-Rad).

Firefly dual-luciferase reporter assay. The TargetScan (http://www.targetscan.org/) website was used to screen out the

Table I. Demographic and clinical characteristic of the patients studied.

Number of patients	33
Sex (male/female)	20/13
Median (range)	
Age (years)	50.2 (17-79)
BM blasts (%)	22.4 (2-88)
Type, N (%)	
RAEB-1	7 (21.2%)
RAEB-2	11 (33.3%)
Secondary AML	15 (45.5%)
Cytogenetic/FISH	
5q-	12
8+	2
Normal	19

Table II. Sequences of primers using in RT-qPCR.

Genes	Forward and reverse primers
miR-143	F:5'-TGTGACACTGAGATGAAGCACTG-3'
	R: 5'-TATGGTTGTTCTGCTCTCTGTCTC-3'
U6	F: 5'-ATTGGAACGATACAGAGAAGATT-3'
	R: 5'-GGAACGCTTCACGAATTTG-3'
FasL	F: 5'-TCCCATCCTCCTGACCAC-3'
	R: 5'-TCGTAAACCGCTTCCCTC-3'
Caspase-8	F: 5'-GGAGTCCATTATCCGTAGT-3'
	R: 5'-AGTTTGAGGGTCTGCTTT-3'
Caspase-3	F: 5'-ATGACATCTCGGTCTGGT-3'
	R: 5'-AGAAACATCACGCATCAA-3'
Caspase-9	F: 5'-CCAAGCCTCTTCTTACTTCACC-3'
	R: 5'-CATCGTTCTGCCATCACTCA-3'
Actin	F: 5'-CCACGAAACTACCTTCAACTAA-3'
	R: 5'-GTGATCTCCTTCTGCATCCTGT-3'

downstream target genes that may be associated with miR-143 and to select the one we were interested in for validation. The wild-type and mutated 3'-UTR fragment from MLLT3/AF9 mRNA was cloned into dual luciferase reporter vectors (Promega, Madison, WI, USA). 293T cells were seeded into 24-well plates and were transfected with negative control vectors, miR-143 mimics (miR-143 inhibitors or a precursor control) and pMIR-MLLT3-WT (or a mutated version of pMIR-MLLT3-Mut), together with the luciferase-reporter vectors. After 2 days of transfection, the Dual-Luciferase Reporter Assay system (Promega) was used to detect the luciferase activity according to the manufacturer's instructions.

SKM-1 xenograft tumour assay. Non-obese diabetic severely compromised immunodeficient (NOD/SCID) mice are ideal models for *in vivo* experiments of blood system tumours, as they have a wide range of immunodeficiencies, such as a lack of functional lymphocytes, low levels of serum immunoglobulin, reduced natural killer (NK) cell activity, dysfunction of antigen-presenting cells, a lack of circulating complement, less rejection and graft anti-host disease (26). NOD/SCID mice are generated by backcrossing SCID mice with non-obese diabetic mice (NOD/Lt). Currently, subcutaneous injections (27) are commonly used for the establishment of blood tumours.

Following approval from the Ethics Committee of the First Affiliated Hospital of Chongqing Medical University, 5- to 6-week-old female NOD/SCID mice (21.57±0.89 g) were purchased from Beijing HFK Bioscience and bred at the Experimental Animal Centre at Chongqing Medical University. Briefly, 15 mice were randomly divided into 3 groups (5 mice per group) as follows: LV-miR-143-treated SKM-1 cells, LV-control-treated SKM-1 cells and untreated SKM-1 cells. To generate subcutaneous xenografts, $2x10^7$ SKM-1 cells suspended in a total volume of 200 μl (PBS pre-chilled to 4˚C) were injected into the right flanks of each mouse. The tumour volume was measured with a calliper every 3 days using the following formula: Volume (mm^3) =L x W^2/2 (L represents the largest diameter, while W is the smallest diameter of the tumour). At the end of the 28-day observation period, the mice were sacrificed. The weight of the mice upon sacrifice was 24.2±1.49 g, the maximum tumour diameter of a single tumour was 1.5 cm and no mouse developed multiple tumours in this study. The tumour tissues were harvested and preserved in 4% paraformaldehyde buffer for histological analyses (28).

Histological analyses. The xenograft tumour tissues were fixed in 4% paraformaldehyde solution, paraffin-embedded and cut into 3-μm-thick sections. The paraffin sections were then stained with haematoxylin and eosin (H&E). Immunohistochemistry for FasL and caspase-3 was performed on two sets of xenograft tissues from each group using a standard technique (29). One set of slides was incubated with the FasL antibody (cat. no. 13098-1-AP, 1:500 dilution, rabbit polyclonal; Proteintech Group, Inc., Chicago, IL, USA), whilst the other set was incubated with the caspase-3 antibody (cat. no. 66470-2-lg, 1:500 dilution, rabbit polyclonal; Proteintech) in Normal Antibody Diluent (ScyTek, phosphate-buffered). The reaction was developed using the protocol of Histostain™-Plus kits (ZSGB-BIO) and counterstained with haematoxylin. Apoptosis was also assessed in situ using the terminal deoxynucleotidyl transferase (TdT) dUTP Nick-End Labeling (TUNEL) apoptosis detection kit (cat. no. C1089, Beyotime) according to the manufacturer's instructions. Cell counting were performed in 3 random fields of each section and cells with dark brown cores were identified as apoptotic cells. The results showed as a percentage of apoptotic cells.

Statistical analysis. All statistical analyses were conducted using SPSS 20.0 software (IBM, Chicago, IL, USA). The results are presented as the means ± standard deviation (SD). A two-tailed Student's t-test was carried out to determine significance when only 2 groups were compared. Variations between groups were analysed with a one-way ANOVA, followed by Tukey's multiple comparison test. Values of $P<0.05$ and $P<0.01$ were considered to indicate statistically significant differences and highly statistically significant differences, respectively.

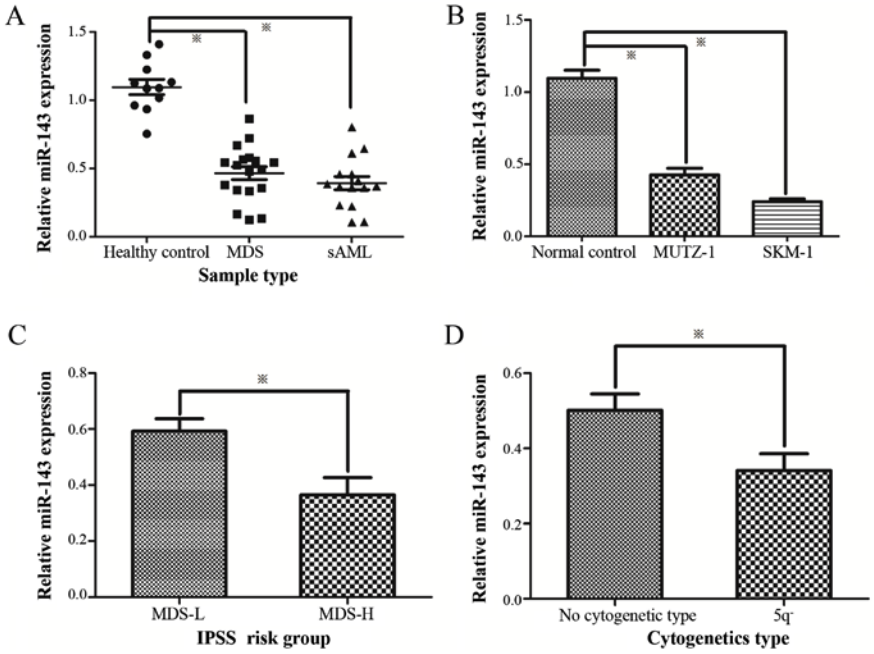

Figure 1. Decreased miR-143 expression levels in BM samples from patients with myelodysplastic syndrome (MDS) and acute myeloid leukaemia (AML) cell lines. (A) RT-qPCR was performed for miR-143 on BM samples from 11 healthy controls, 18 MDS patients and 15 secondary AML patients (sAML). (B) RT-qPCR analysis of the differential expression levels of miR-143 between healthy controls and MDS/AML cell lines (SKM-1). (C) Association analysis of miR-143 expression levels in risk stratification. (D) Analysis of miR-143 expression levels in the cytogenetic type. *P<0.05.

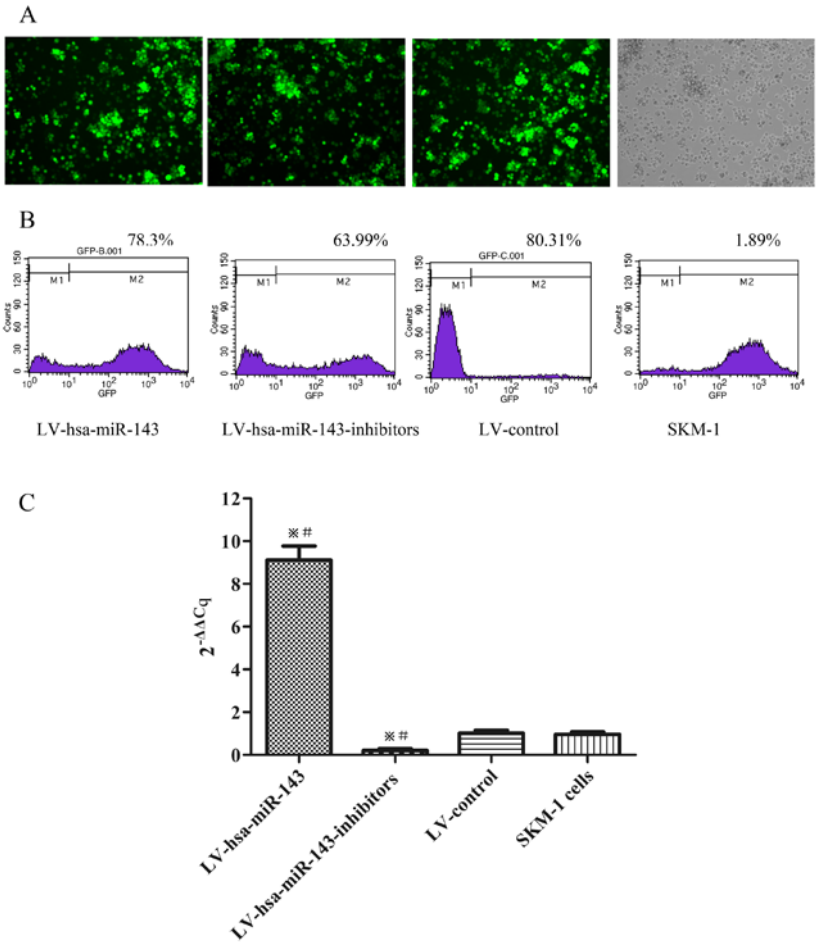

Figure 2. SKM-1 cells were transfected with lentiviral vectors, and the infection efficiency was detected. (A) Follwoing transfection, green fluorescent protein (GFP) was observed under a fluorescence microscope with the control group under white light (magnification, x400). (B) The infection rates were detected by flow cytometry, with the infection rate of LV-hsa-miR-143 being 78.3%, the LV-hsa-miR-143-inhibitors being 63.99%, the negative control 80.31% and SKM-1 cells 1.89%. P2 represents GFP. (C)RT-qPCR analysis of the expression levels of miR-143 in each group. *P<0.05 vs. LV-control, #P<0.05 vs. SKM-1.

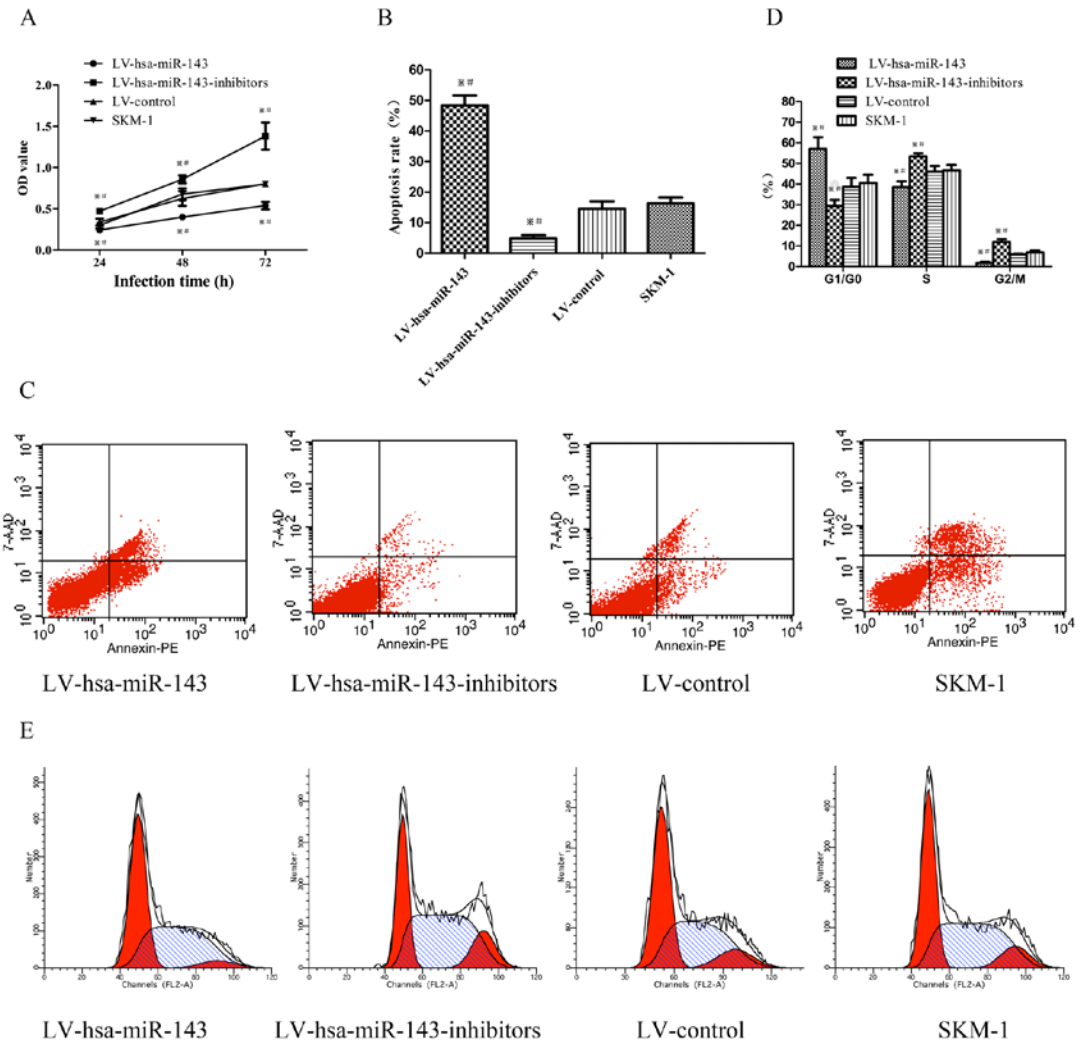

Figure 3. miR-143 inhibits the proliferation and induces the apoptosis and cell cycle arrest of SKM-1 cells. (A) SKM-1 cells were transfected with LV-hsa-miR-143, LV-hsa-miR-143-inhibitors, LV-control and negative control (SKM-1 cells), and the rate of cell proliferation was measured with a CCK-8 assay. (B and C) Flow cytometric analysis of apoptosis in each group. (D and E) Cell cycle analysis of SKM-1 cells transfected with each lentiviral vector evaluated by flow cytometry. *P<0.05 vs. LV-control, #P<0.05 vs. SKM-1.

Results

miR-143 expression levels are decreased in MDS/AML samples and cell lines. The expression levels of miR-143 in 33 patients with MDS/AML and SKM-1 were compared to those of 11 healthy controls. Following normalization and data calculations, miR-143 expression was found to be significantly decreased in MDSand secondary AML (sAML) samples and cell lines compared to the healthy controls (Fig. 1A and B). Compared to the low-risk MDS group, the expression of miR-143 was evidently decreased in the high-risk MDS group (Fig. 1C). Moreover, the miR-143 expression levels in patients with MDS with the 5q deletion were significantly lower than the normal cytogenetic type (Fig. 1D).

Recombinant lentiviral vectors lead to variations in the miR-143 levels in SKM-1 cells. To clarify the role of miR-143 in MDS, the SKM-1 cells were transfected with LV-hsa-miR-143 and LV-hsa-miR-143-inhibitors, respectively. The infection efficiency was evaluated using a fluorescence microscope (Fig. 2A) and flow cytometry, with >60% of the SKM-1 cells being positive for green fluorescent protein (GFP) (Fig. 2B). miR-143 expression was then detected by RT-qPCR. Compared to the LV-control and the normal control (SKM-1 cells), LV-hsa-miR-143 induced the upregulation of miR-143 expression 9-fold, whereas LV-hsa-miR-143-inhibitors downregulated the expression of miR-143 by approximately a quarter (Fig. 2C).

miR-143 affects the proliferation, apoptosis and cell cycle of SKM-1 cells. To assess the role of miR-143 in the SKM-1 cells following transfection, a CCK-8 assay was used to evaluate the effects of miR-143 on the proliferation of SKM-1 cells. The optical density (OD) value of the cells transfected with LV-hsa-mir-143 was significantly lower than that of the negative control and SKM-1 cells, whereas the OD of cells transfected with LV-hsa-miR-143-inhibitors was higher than control groups (Fig. 3A). The apoptotic rate of the SKM-1 cells transfected with LV-hsa-mir-143 demonstrated a significant 3-fold increase, while the apoptotic rate of the cells transfected with LV-hsa-miR-143-inhibitors was decreased by more than half, compared to the control groups (Fig. 3B and C). Furthermore, the cell cycle profile was examined by flow cytometry. The

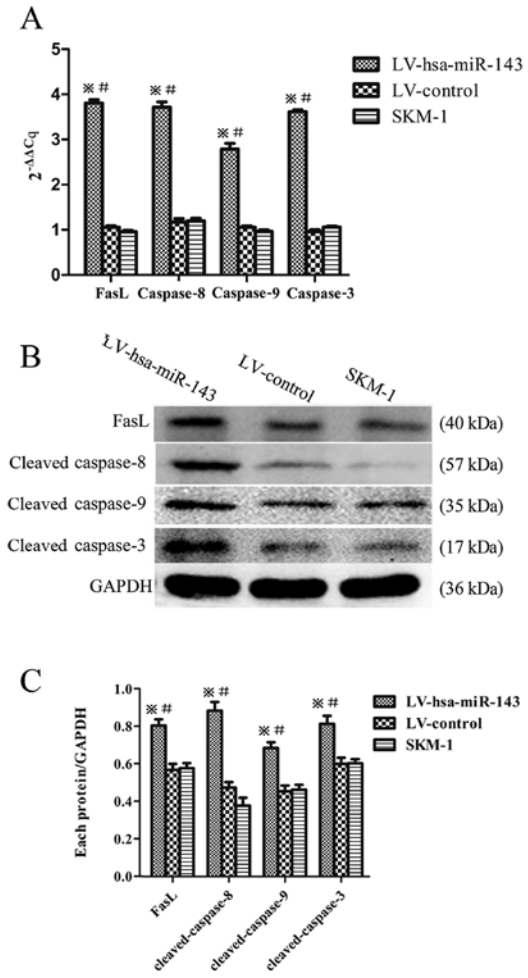

Figure 4. Overexpression of miR-143 regulates SKM-1 cells via the Fas/FasL pathway. (A) Changes in the expression levels of FasL, caspase-8, caspase-9 and caspase-3 as determined by RT-qPCR. (B and C) Analysis of the expression levels of FasL, cleaved caspase-8, cleaved caspase-9 and cleaved caspase-3 determined by western blot analysis. *P<0.05 vs. LV-control, #P<0.05 vs. SKM-1.

number of SKM-1 cells transfected with LV-hsa-miR-143 arrested in the G1/G0 phase increased by >16%, while that of the cells transfected with LV-hsa-miR-143-inhibitors decreased by 10% compared to the control groups (Fig. 3D and E). Taken together, these results suggest that miR-143 inhibits the proliferation, and induces the apoptosis and cell cycle arrest of SKM-1 cells.

The overexpression of miR-143 activates the Fas/FasL apoptotic pathway. To further examine the specific mechanisms of the miR-143-induced apoptosis in SKM-1 cells, RT-qPCR (Fig. 4A) and western blot analysis (Fig. 4B and C) were employed for the detection of FasL, cleaved caspase-8, -9 and -3. An increased expression of the apoptotic factors, caspase-8, -3 and -9 and FasL at both the mRNA and protein level compared to the LV-control and SKM-1 cells was observed, confirming that miR-143 overexpression activates the Fas/FasL apoptotic pathway.

LV-hsa-miR-143 binds to the 3'-UTR of AF9 and inhibits its expression. To further elucidate the possible molecular mechanisms involved, the target prediction website, Targetscan was utilised (30). Bioinformatics analyses indicated that the MLLT3/AF9 gene was a putative target of miR-143 (Fig. 5A). We conducted a Firefly luciferase reporter assay to clarify whether AF9 is a direct target of miR-143. The luciferase reporter containing the AF9 3'-UTR was significantly suppressed by miR-143, whereas the mutated reporter was not affected (Fig. 5B). Subsequently, miR-143 inhibitors and pMIR-MLLT3-WT vector were transfected into the SKM-1 cells, with results demonstrating that miR-143 inhibitors can increase luciferase activity, hence indicating that LV-hsa-miR-143 binds to the 3'-UTR of AF9 and inhibits its expression (Fig. 5C). Furthermore, western blot analysis was performed to determine whether the knockdown miR-143 led

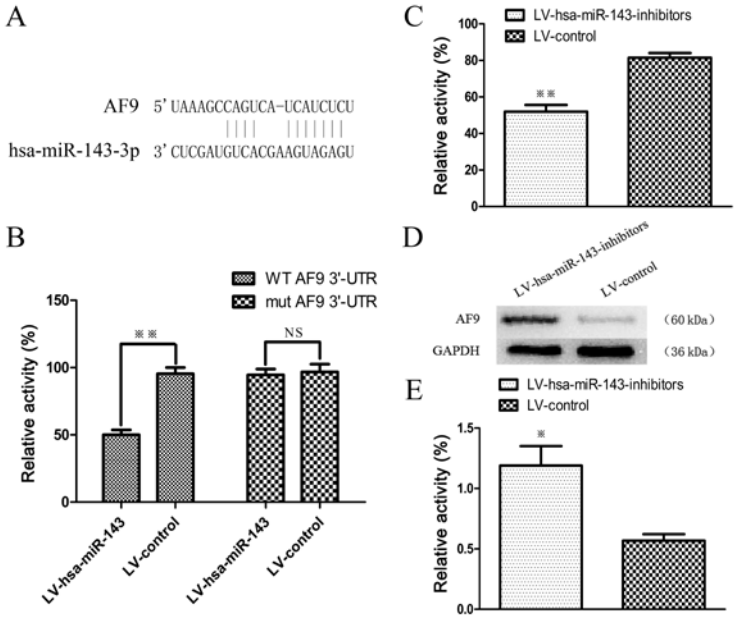

Figure 5. miR-143 directly targets the 3'-UTR of MLLT3/AF9 to suppress its expression in SKM-1 cells. (A) 3'-UTR of AF9 with seed region and base substitutions. (B) Enforced miR-143 expression inhibited the luciferase activity of the wild-type (WT), but not the mutated (MUT) 3'-UTR reporter. (C and D) Analysis of the protein expression levels of the MLLT3/AF9 determined by western blot analysis. NS, not statistically significant; *P<0.05 vs. LV-control, **P<0.01 vs. LV-control.

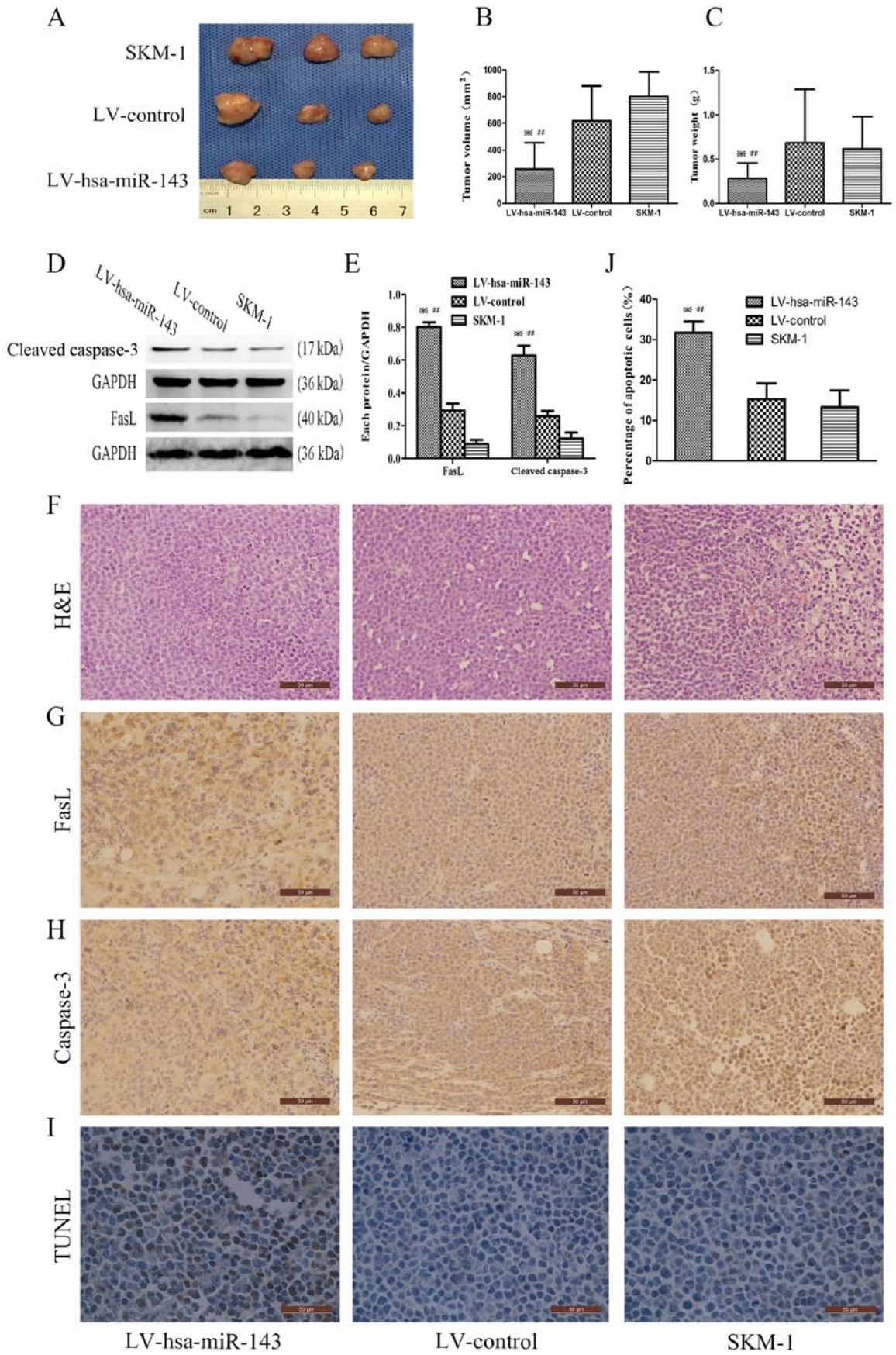

Figure 6. The effect of miR-143 on SKM-1 cell-derived tumour growth. (A) Images of tumours obtained from NOD/SCID mice in each group. (B and C) Both the volume and weight of xenograft tumours was decreased in the miR-143-overexpressing group compared to the two control groups. (D and E) The expression of FasL and cleaved caspase-3 in tumour tissue was evaluated by western blot analysis. GAPDH was used as a loading control. (F) H&E staining of the tumour xenografts in each group (magnification, x400). (G) Immunohistochemical staining of the FasL antigen of the tumour xenografts in each group magnification, x400). (H) Immunohistochemical staining of the caspase-3 antigen of the tumour xenografts in each group (magnification, x400). (I) Representative images of TUNEL staining (magnification, x400). Cell with deep brown nuclei was identified as TUNEL-positive cells. *P<0.05 vs. LV-control, $^{\#}$P<0.05 vs. SKM-1.

to an upregulation of MLLT3/AF9 expression (Fig. 5D and E). The results revealed that AF9 was a target of and regulated by miR-143.

Overexpression of miR-143 inhibits tumour growth and promotes apoptosis in vivo. To verify the function of miR-143 in tumour growth in the complex microenvironment, NOD/SCID mice were subcutaneously injected with LV-hsa-miR-143 SKM-1 cells, LV-control SKM-1 cells or untreated SKM-1 cells. Consistent with the *in vitro* findings, tumours derived from SKM-1 cells overexpressing miR-143 exhibited significantly reduced growth (Fig. 6A-C). Western blot analysis was employed for the detection of FasL and cleaved caspase-3 in the tumour samples, with the results demonstrating that the overexpression of miR-143 enhanced the expression of FasL and cleaved caspase-3 compared to that in the SKM-1 cell group (Fig. 6D and E). H&E staining of the xenograft tumours revealed unsystematic and irregular tumour cell arrangements and an increased the nuclear-cytoplasmic ratio, which is consistent with the pathological characteristics of malignancy (Fig. 6F). The results of immunohistochemical staining revealed that both FasL and caspase-3 were strongly positive in the LV-hsa-miR-143 group (Fig. 6G). Moreover, a TUNEL assay was performed, which revealed that the proportion of apoptotic cells was higher in the LV-hsa-miR-143 group (31.71±2.78%) than in the LV-control group (15.32±3.91%, $P<0.001$) or the untreated SKM-1 cell group (13.29±4.15%, $P<0.001$, Fig. 6I and J). Taken together, these results confirm that the overexpression of miR-143 activates the FasL apoptotic pathway.

Discussion

Recent studies have demonstrated that miR-143 plays an inhibitory role in different tumours types and has a significant effect on the haematopoietic system (31,32). To further support these findings, the results of the present study suggested that the overexpression of miR-143 significantly inhibited AML cell proliferation. Additionally, we also demonstrated that the downregulation of miR-143 significantly promoted cell proliferation, suggesting that miR-143 is likely an anticancer factor for MDS/AML. To further elucidate the mechanisms through which miR-143 inhibits SKM-1 cell proliferation, flow cytometric analysis was performed to assess the cell cycle profile, with an increased cell number of cells in the LV-hsa-miR-143 group in the G0/G1 phase and a decreased number in the S phase being observed. By contrast, the LV-hsa-miR-143-inhibitors group exhibited favorable conditions for cell apoptosis in the G0/G1 phase. Therefore, it can be concluded that miR-143 inhibits AML cell proliferation, promotes apoptosis and arrests cell growth cycle at the G0/G1 phase.

To verify whether the *in vitro* effects of miR-143 on MDS reflect the *in vivo* response, experiments using NOD/SCID mice which were subcutaneously injected with SKM-1 cells stably expressing miR-143 were performed. The results indicated that the upregulation of miR-143 expression increased apoptosis through the activation of the FasL pathway, thereby attenuating the growth of the tumour xenografts. Furthermore, these findings provide evidence that the overexpression of miR-143 promotes the apoptosis of SKM-1 cells by activating the Fas/FasL signalling pathway. To further explore the mechanisms through which miR-143 overexpression promotes apoptosis, the MLLT3/AF9 gene was selected using the TargetScan online bioinformatics tool, which predicts biological targets of miRNAs by searching for the presence of conserved 8mer, 7mer and 6mer sites matching the seed region of each miRNA (33). MLLT3/AF9 is a proto-oncogene capable of relieving the expression of key genes in leukaemia, and it may be a key regulator of lymphoma cell proliferation or carcinogenesis (34-36). As described herein, both a wild-type and mutant vector of the MLLT3/AF9 3'-UTR were constructed and inhibition was verified with a Firefly luciferase reporter gene assay. The results demonstrated that miR-143 analogues inhibited wild-type MLLT3/AF9, whereas the mutant remaind unaffected, thus confirming the status of the MLLT3/AF9 gene as a target gene of miR-143.

Taken together, the findings of this study suggest that miR-143 overexpression inhibits the proliferation of SKM-1 cells both *in vitro* and *in vivo*. This may be due to miR-143 affecting the apoptotic pathway of FasL, hence supporting the use of MLLT3/AF9 inhibitors as potential antitumour therapy for MDS, whose effects need to be extensively confirmed by clinical trials.

Acknowledgements

The authors would like to thank Mr. Peng etc. from The Chongqing Key Laboratory of Translational Medicine in Major Metabolic Diseases for providing assistance with the experiments. The MDS/AML cell line SKM-1 cells were kindly provided by Professor Jianfeng Zhou of Tongji Medical College of Huazhong University of Science and Technology (Wuhan, China).

Funding

This study was supported by the Chongqing Education Commission Foundation (KJ1702017) and the National Natural Science Foundation of China (grant nos. 30971277 and 81250034).

Availability of data and materials

The datasets used and/or analyzed during the current study are available from the corresponding author on reasonable request.

Authors' contributions

CW and CP performed the molecular experiments and drafted the manuscript. JC and LD performed the *in vivo* assays. XK took part in data collection and processing. ZZ was responsible for the preparation of pathological sections and immunohistochemistry. JC and LW were responsible for the conception and design of the study and manuscript revision. All authors have read and approved the final manuscript.

Ethics approval and consent to participate

All clinical samples were collected by the informed consent signed by the patients and approved by the Institutional Review

Board of The First Affiliated Hospital of Chongqing Medical University. Animal handling and procedures were approved by the Ethics Committee of the First Affiliated Hospital of Chongqing Medical University.

Patient consent for publication

Not applicable.

Competing interests

The authors declare that they have no competing interests.

References

1. de Witte T, Bowen D, Robin M, Malcovati L, Niederwieser D, Yakoub-Agha I, Mufti GJ, Fenaux P, Sanz G, Martino R, *et al*: Allogeneic hematopoietic stem cell transplantation for MDS and CMML: Recommendations from an international expert panel. Blood 129: 1753-1762, 2017.
2. Pellagatti A and Boultwood J: The molecular pathogenesis of the myelodysplastic syndromes. Eur J Haematol 95: 3-15, 2015.
3. Mandal N: Bibliometric analysis of global publication output and collaboration structure study in microRNA research. Scientometrics 98: 2011-2037, 2014.
4. Kuang X, Chi J and Wang L: Deregulated microRNA expression and its pathogenetic implications for myelodysplastic syndromes. Hematology 21: 593-602, 2016.
5. Simmer F, Venderbosch S, Dijkstra JR, Vink-Börger EM, Faber C, Mekenkamp LJ, Koopman M, De Haan AF, Punt CJ and Nagtegaal ID: MicroRNA-143 is a putative predictive factor for the response to fluoropyrimidine-based chemotherapy in patients with metastatic colorectal cancer. Oncotarget 6: 22996-23007, 2015.
6. Hu Y, Ma Z, He Y, Liu W, Su Y and Tang Z: PART-1 functions as a competitive endogenous RNA for promoting tumor progression by sponging miR-143 in colorectal cancer. Biochem Biophys Res Commun 490: 317-323, 2017.
7. Yu B, Liu X and Chang H: MicroRNA-143 inhibits colorectal cancer cell proliferation by targeting MMP7. Minerva Med 108: 13-19, 2017.
8. Zhou P, Chen WG and Li XW: MicroRNA-143 acts as a tumor suppressor by targeting hexokinase 2 in human prostate cancer. Am J Cancer Res 5: 2056-2063, 2015.
9. Rodríguez M, Bajo-Santos C, Hessvik NP, Lorenz S, Fromm B, Berge V, Sandvig K, Linē A and Llorente A: Identification of non-invasive miRNAs biomarkers for prostate cancer by deep sequencing analysis of urinary exosomes. Mol Cancer 16: 156, 2017.
10. Wang F, Liu J, Zou Y, Jiao Y, Huang Y, Fan L, Li X, Yu H, He C, Wei W, *et al*: MicroRNA-143-3p, up-regulated in H. pylori-positive gastric cancer, suppresses tumor growth, migration and invasion by directly targeting AKT2. Oncotarget 8: 28711-28724, 2017.
11. Du F, Feng Y, Fang J and Yang M: MicroRNA-143 enhances chemosensitivity of Quercetin through autophagy inhibition via target GABARAPL1 in gastric cancer cells. Biomed Pharmacother 74: 169-177, 2015.
12. Li J, Wang X, Zhang Y and Zhang Y: E3 ubiquitin ligase isolated by differential display regulates cervical cancer growth in vitro and in vivo via microRNA-143. Exp Ther Med 12: 676-682, 2016.
13. Dong P, Xiong Y, Hanley SJB, Yue J and Watari H: Musashi-2, a novel oncoprotein promoting cervical cancer cell growth and invasion, is negatively regulated by p53-induced miR-143 and miR-107 activation. J Exp Clin Cancer Res 36: 150, 2017.
14. Chen JH, Yang R, Zhang W and Wang YP: Functions of microRNA-143 in the apoptosis, invasion and migration of nasopharyngeal carcinoma. Exp Ther Med 12: 3749-3755, 2016.
15. He B, Xu Z, Chen J, Zheng D, Li A and Zhang LS: Upregulated microRNA-143 inhibits cell proliferation in human nasopharyngeal carcinoma. Oncol Lett 12: 5023-5028, 2016.
16. Li WH, Wu HJ, Li YX, Pan HG, Meng T and Wang X: MicroRNA-143 promotes apoptosis of osteosarcoma cells by caspase-3 activation via targeting Bcl-2. Biomed Pharmacother 80: 8-15, 2016.
17. Zhang H, Wang G, Ding C, Liu P, Wang R, Ding W, Tong D, Wu D, Li C, Wei Q, *et al*: Increased circular RNA UBAP2 acts as a sponge of miR-143 to promote osteosarcoma progression. Oncotarget 8: 61687-61697, 2017.
18. Akao Y, Nakagawa Y, Iio A and Naoe T: Role of microRNA-143 in Fas-mediated apoptosis in human T-cell leukemia Jurkat cells. Leuk Res 33: 1530-1538, 2009.
19. Ozdogan H, Gur Dedeoglu B, Oztemur Islakoglu Y, Aydos A, Kose S, Atalay A, Yegin ZA, Avcu F, Uckan Cetinkaya D and Ilhan O: DICER1 gene and miRNA dysregulation in mesenchymal stem cells of patients with myelodysplastic syndrome and acute myeloblastic leukemia. Leuk Res 63: 62-71, 2017.
20. Votavova H, Grmanova M, Dostalova Merkerova M, Belickova M, Vasikova A, Neuwirtova R and Cermak J: Differential expression of microRNAs in $CD34^+$ cells of 5q- syndrome. J Hematol Oncol 4: 1, 2011.
21. Dostalova Merkerova M, Krejcik Z, Votavova H, Belickova M, Vasikova A and Cermak J: Distinctive microRNA expression profiles in $CD34^+$ bone marrow cells from patients with myelodysplastic syndrome. Eur J Hum Genet 19: 313-319, 2011.
22. Wang L, Luo J, Nian Q, Xiao Q, Yang Z and Liu L: Ribosomal protein S14 silencing inhibits growth of acute myeloid leukemia transformed from myelodysplastic syndromes via activating p53. Hematology 19: 225-231, 2014.
23. Liu Z, Ding K, Li L, Liu H, Wang Y, Liu C and Fu R: A novel histone deacetylase inhibitor Chidamide induces G0/G1 arrest and apoptosis in myelodysplastic syndromes. Biomed Pharmacother 83: 1032-1037, 2016.
24. Livak KJ and Schmittgen TD: Analysis of relative gene expression data using real-time quantitative PCR and the 2(-Delta Delta C(T)) Method. Methods 25: 402-408, 2001.
25. Tiscornia G, Singer O and Verma IM: Production and purification of lentiviral vectors. Nat Protoc 1: 241-245, 2006.
26. Proetzel G and Wiles MV (eds.): Mouse Models for Drug Discovery: Methods and Protocols. Humana Press, Totowa, NJ, 2010.
27. Wu L, Li X, Su J, He Q, Zhang X, Chang C and Pu Q: Efficacy and safety of CHG regimen (low-dose cytarabine, homoharringtonine with G-CSF priming) as induction chemotherapy for elderly patients with high-risk MDS or AML transformed from MDS. J Cancer Res Clin Oncol 137: 1563-1569, 2011.
28. Pramanik D, Campbell NR, Karikari C, Chivukula R, Kent OA, Mendell JT and Maitra A: Restitution of tumor suppressor microRNAs using a systemic nanovector inhibits pancreatic cancer growth in mice. Mol Cancer Ther 10: 1470-1480, 2011.
29. Guerenne L, Beurlet S, Said M, Gorombei P, Le Pogam C, Guidez F, de la Grange P, Omidvar N, Vanneaux V, Mills K, *et al*: GEP analysis validates high risk MDS and acute myeloid leukemia post MDS mice models and highlights novel dysregulated pathways. J Hematol Oncol 9: 5, 2016.
30. Agarwal V, Bell GW, Nam JW and Bartel DP: Predicting effective microRNA target sites in mammalian mRNAs. eLife 4: 4, 2015.
31. Zhou J, Chaudhry H, Zhong Y, Ali MM, Perkins LA, Owens WB, Morales JE, McGuire FR, Zumbrun EE, Zhang J, *et al*: Dysregulation in microRNA expression in peripheral blood mononuclear cells of sepsis patients is associated with immunopathology. Cytokine 71: 89-100, 2015.
32. Shen JZ, Zhang YY, Fu HY, Wu DS and Zhou HR: Overexpression of microRNA-143 inhibits growth and induces apoptosis in human leukemia cells. Oncol Rep 31: 2035-2042, 2014.
33. Lewis BP, Burge CB and Bartel DP: Conserved seed pairing, often flanked by adenosines, indicates that thousands of human genes are microRNA targets. Cell 120: 15-20, 2005.
34. Chen X, Clark J, Wunderlich M, Fan C, Davis A, Chen S, Guan JL, Mulloy JC, Kumar A and Zheng Y: Autophagy is dispensable for Kmt2a/Mll-Mllt3/Af9 AML maintenance and anti-leukemic effect of chloroquine. Autophagy 13: 955-966, 2017.
35. Zhang T, Luo Y, Wang T and Yang JY: MicroRNA-297b-5p/3p target Mllt3/Af9 to suppress lymphoma cell proliferation, migration and invasion in vitro and tumor growth in nude mice. Leuk Lymphoma 53: 2033-2040, 2012.
36. Vogel T and Gruss P: Expression of leukaemia associated transcription factor Af9/Mllt3 in the cerebral cortex of the mouse. Gene Expr Patterns 9: 83-93, 2009.